Revealing nonclassicality beyond Gaussian states via a single marginal distribution

Jiyong Park[a], Yao Lu[b], Jaehak Lee[a], Yangchao Shen[b], Kuan Zhang[b], Shuaining Zhang[b], Muhammad Suhail Zubairy[c], Kihwan Kim[b], and Hyunchul Nha[a,1]

[a]Department of Physics, Texas A&M University at Qatar, Education City, Doha, Qatar; [b]Center for Quantum Information, Institute for Interdisciplinary Information Sciences, Tsinghua University, Beijing 100084, People's Republic of China; and [c]Department of Physics and Institute of Quantum Studies, Texas A&M University, College Station, TX 77843

Edited by Luiz Davidovich, Federal University of Rio de Janeiro, Rio de Janeiro, Brazil, and approved December 13, 2016 (received for review October 25, 2016)

A standard method to obtain information on a quantum state is to measure marginal distributions along many different axes in phase space, which forms a basis of quantum-state tomography. We theoretically propose and experimentally demonstrate a general framework to manifest nonclassicality by observing a single marginal distribution only, which provides a unique insight into nonclassicality and a practical applicability to various quantum systems. Our approach maps the 1D marginal distribution into a factorized 2D distribution by multiplying the measured distribution or the vacuum-state distribution along an orthogonal axis. The resulting fictitious Wigner function becomes unphysical only for a nonclassical state; thus the negativity of the corresponding density operator provides evidence of nonclassicality. Furthermore, the negativity measured this way yields a lower bound for entanglement potential—a measure of entanglement generated using a nonclassical state with a beam-splitter setting that is a prototypical model to produce continuous-variable (CV) entangled states. Our approach detects both Gaussian and non-Gaussian nonclassical states in a reliable and efficient manner. Remarkably, it works regardless of measurement axis for all non-Gaussian states in finite-dimensional Fock space of any size, also extending to infinite-dimensional states of experimental relevance for CV quantum informatics. We experimentally illustrate the power of our criterion for motional states of a trapped ion, confirming their nonclassicality in a measurement-axis–independent manner. We also address an extension of our approach combined with phase-shift operations, which leads to a stronger test of nonclassicality, that is, detection of genuine non-Gaussianity under a CV measurement.

nonclassicality | non-Gaussianity | continuous variable | quantum entanglement

Nonclassicality is a fundamentally profound concept to identify quantum phenomena inaccessible from classical physics. It also provides a practically useful resource, for example, entanglement, making possible a lot of applications in quantum information processing beyond classical counterparts (1–3). A wide range of quantum systems, for example, field amplitudes of light, collective spins of atomic ensembles, motional modes of trapped ions, and Bose–Einstein condensate and mechanical oscillators, can be used for quantum information processing based on continuous variables (CVs) (2). It is of crucial importance to establish efficient and reliable criteria of nonclassicality for CV systems, desirably testable with fewer experimental resources, for example, fewer measurement settings (4–8) and with the capability of detecting a broad class of nonclassical states. In this paper, in view of the Glauber–Sudarshan P function (9, 10), those states that cannot be represented as a convex mixture of coherent states are referred to as nonclassical.

A standard method to obtain information on a CV quantum state is to measure marginal distributions along many different axes in phase space constituting quantum-state tomography (11). This tomographic reconstruction may reveal nonclassicality to some extent, for example, negativity of Wigner function making only a subset of whole nonclassicality conditions. However, it typically suffers from a legitimacy problem; that is, the measured distributions do not yield a physical state when directly used due to finite data and finite binning size (11, 12). Much efforts was made to use estimation methods finding a most probable quantum state closest to the obtained data (13–16). There were also numerous studies to directly detect nonclassicality, for example, an increasingly large number of hierarchical conditions (4) requiring information on two or more marginal distributions or measurement of many higher-order moments (17–19). An exception would be the case of Gaussian states, with its nonclassical squeezing demonstrated by the variance of distribution along a squeezed axis.

Here we theoretically propose and experimentally demonstrate a simple, powerful, method to directly manifest nonclassicality by observing a single marginal distribution applicable to a wide range of nonclassical states. Our approach makes use of a phase-space map that transforms the marginal distribution (obtained from measurement) to a factorized Wigner distribution by multiplying the same distribution or the vacuum-state distribution along an orthogonal axis. We refer to those mathematical procedures as demarginalization maps (DMs), because a one-dimensional marginal distribution is converted to a fictitious

Significance

Quantum states possess nonclassical properties inaccessible from classical physics, providing a profound basis of quantum physics and a crucial resource for quantum information technology. We propose a general framework to manifest nonclassicality via single marginal distributions, unlike quantum-state tomography using many marginal distributions, applicable to a broad range of quantum systems. Our approach provides a fundamentally unique insight showing how partial information on a quantum state can be sufficient to confirm nonclassicality and a practical efficiency, yielding conclusive evidence of nonclassicality by directly analyzing experimental data without numerical optimization. Remarkably, our method works regardless of measurement axis for all non-Gaussian states of finite dimension. We also experimentally demonstrate our framework, using motional states of a trapped ion.

Author contributions: J.P. and H.N. designed research; J.P., J.L., M.S.Z., and H.N. developed theory; Y.L., Y.S., K.Z., S.Z., and K.K. performed the experiment; J.P. and H.N. analyzed experimental data; J.P., K.K., and H.N. wrote the paper; and H.N. supervised the project.

The authors declare no conflict of interest.

This article is a PNAS Direct Submission.

Freely available online through the PNAS open access option.

[1]To whom correspondence should be addressed. Email: hyunchul.nha@qatar.tamu.edu.

This article contains supporting information online at www.pnas.org/lookup/suppl/doi:10.1073/pnas.1617621114/-/DCSupplemental.

2D Wigner function. The same method can be applied equally to the characteristic function as well as the Wigner function. We show that a classical state, that is, a mixture of coherent states, must yield a physical state under our DMs. That is, the unphysicality emerging under DMs is a clear signature of nonclassicality. Remarkably, for all non-Gaussian states in finite-dimensional space, our test works for an arbitrary single marginal distribution thus experimentally favorable. (For Gaussian states, our method, if directly applied, works only for the squeezed axes not covering the whole range of quadrature axis. As we show in *SI Appendix*, however, a phase randomization, which does not create nonclassicality, modifies a Gaussian state to a non-Gaussian state for which nonclassicality can be detected regardless of quadrature axis.) It also extends to non-Gaussian states in infinite dimension, particularly those without squeezing effect. We introduce a quantitative measure of nonclassicality using our DMs, which provides a lower bound of entanglement potential (20)—an entanglement measure under a beam-splitter setting versatile for CV entanglement generation (20–23). Along this way, our method makes a rigorous connection between single-mode nonclassicality and negative partial transpose (NPT) entanglement (24–33), which bears on entanglement distillation (34) and nonlocality (35–42).

As the measurement of a marginal distribution is highly efficient in various quantum systems, for example, homodyne detection in quantum optics, our proposed approach can provide a practically useful and reliable tool in a wide range of investigations for CV quantum physics. We here experimentally illustrate the power of our approach by manifesting nonclassicality of motional states in a trapped-ion system. Specifically, we confirm the nonclassicality regardless of measured quadrature axis by introducing a simple faithful test using only a subset of data points, not requiring data manipulation under numerical methods, unlike the case of state reconstruction. We also extend our approach combined with phase randomization to obtain a criterion on genuine non-Gaussianity.

DMs and Nonclassicality Measure

Nonclassicality Test via DMs. We first introduce our main tools, that is, DMs,

$$\mathcal{D}_1 : W_\rho(q,p) \mapsto M_\rho(x)M_\rho(y) \equiv W_\rho^{\mathrm{DM1}}(x,y), \qquad [1]$$

$$\mathcal{D}_2 : W_\rho(q,p) \mapsto M_\rho(x)M_{|0\rangle\langle 0|}(y) \equiv W_\rho^{\mathrm{DM2}}(x,y), \qquad [2]$$

where $(x,y)^T = \mathcal{R}(\theta)(q,p)^T$ is a pair of orthogonal quadratures rotated from position q and momentum p with $\mathcal{R}(\theta) = \begin{pmatrix} \cos\theta & \sin\theta \\ -\sin\theta & \cos\theta \end{pmatrix}$. $M_\rho(x) = \int dy W_\rho(x,y)$ is a marginal distribution of the Wigner function $W_\rho(q,p) = \frac{2}{\pi}\mathrm{tr}[\rho\hat{D}(\alpha)(-1)^{\hat{n}}\hat{D}^\dagger(\alpha)]$, where $\hat{D}(\alpha) = e^{\alpha\hat{a}^\dagger - \alpha^*\hat{a}}$ is a displacement operator with $\alpha = q + ip$ (43, 44).

Our DM methods proceed as follows. Given a state with its Wigner function $W_\rho(q,p)$, we measure a marginal distribution $M_\rho(x)$ along a certain axis, $x = q\cos\theta + p\sin\theta$. We then construct a fictitious, factorized, Wigner function $W_\rho^{\mathrm{DM}}(x,y)$ either by replicating the obtained distribution as $M_\rho(x)M_\rho(y)$ (DM1) or by multiplying the marginal distribution of a vacuum state as $M_\rho(x)M_{|0\rangle\langle 0|}(y)$ (DM2), with $M_{|0\rangle\langle 0|}(y) = \sqrt{\frac{2}{\pi}}e^{-2y^2}$ (Fig. 1). We test whether $W_\rho^{\mathrm{DM}}(x,y)$ is a legitimate Wigner function to represent a physical state.

Nonclassicality criteria. The constructed functions in Eqs. **1** and **2** are both in factorized forms, so judging their legitimacy is related to the problem of what quantum states can possess a factorized Wigner function. (Note also that a factorized Wigner function must be everywhere nonnegative as each term in it represents its marginal distribution so is nonnegative.) Every coherent state $|\beta\rangle$ has a factorized Wigner function against all pairs of orthogonal quadratures, $W_{|\beta\rangle\langle\beta|}(x,y) = \frac{2}{\pi}e^{-2(x-\beta_x)^2}e^{-2(y-\beta_y)^2}$ (7). Owing to this factorizability, the maps $\mathcal{D}_1$ and $\mathcal{D}_2$ transform a classical state into another classical one. A mixture of coherent states has a Wigner function

$$W_{\rho_{\mathrm{cl}}}(x,y) = \int d^2\beta P(\beta_x,\beta_y)\, W_{|\beta\rangle\langle\beta|}(x,y), \qquad [3]$$

with the probability density $P(\beta_x,\beta_y)$ for a coherent state $|\beta\rangle$ ($\beta = \beta_x + i\beta_y$). Applying each DM leads to

$$\mathcal{D}_j[W_{\rho_{\mathrm{cl}}}(q,p)] = \int d^2\beta Q_1(\beta_x)Q_j(\beta_y)\, W_{|\beta\rangle\langle\beta|}(x,y) \qquad [4]$$

($j = 1, 2$), where $Q_1(\beta_x) = \int d\beta_y P(\beta_x,\beta_y)$ and $Q_2(\beta_x) = \delta(\beta_x)$ are nonnegative. The resulting distributions in Eq. **4** also represent a certain mixture of coherent states and hence a physical state. Therefore, if an unphysical Wigner function emerges under our DMs, the input state must be nonclassical.

Gaussian states. Let us first consider a Gaussian state σ that has a squeezed quadrature $\hat{x}$ with $V_x \equiv \Delta^2\hat{x} < \frac{1}{4}$. Taking the squeezed marginal $M_\sigma(x) = \frac{1}{\sqrt{2\pi V_x}}e^{-\frac{(x-\langle\hat{x}\rangle)^2}{2V_x}}$ yields

$$\mathcal{D}_1[W_\sigma(q,p)] = \frac{1}{2\pi V_x}e^{-\frac{(x-\langle\hat{x}\rangle)^2}{2V_x}}e^{-\frac{(y-\langle\hat{x}\rangle)^2}{2V_x}},$$

$$\mathcal{D}_2[W_\sigma(q,p)] = \frac{1}{\pi\sqrt{V_x}}e^{-\frac{(x-\langle\hat{x}\rangle)^2}{2V_x}}e^{-2y^2}, \qquad [5]$$

both of which violate the uncertainty relation $\Delta\hat{x}\Delta\hat{y} \geq \frac{1}{4}$. Thus, the squeezed state turns into an unphysical state under our DMs. This method, of course, succeeds only when the observed marginal distribution is along a squeezed axis that generally extends to a finite range of angles, if not the whole range of angles (*SI Appendix*). We can further make the test successful regardless of quadrature axis by introducing a random phase rotation on a Gaussian state (*SI Appendix*). Note that a mixture of phase rotations, which transforms a Gaussian to a non-Gaussian state, does not create nonclassicality, so the nonclassicality detected after phase rotations is attributed to that of the original state.

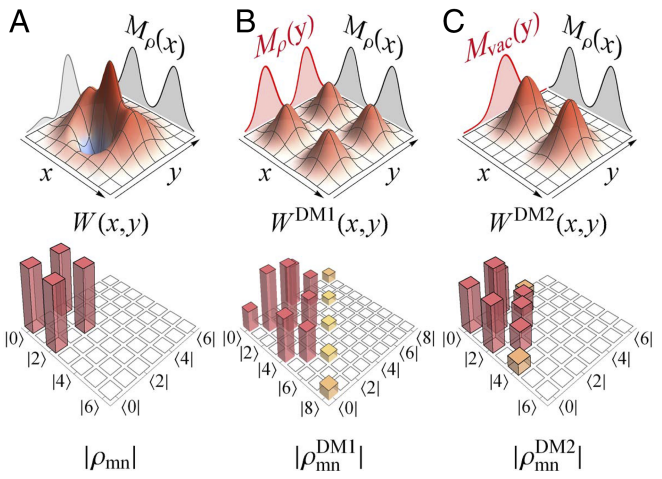

Fig. 1. DMs. (*A*) original Wigner function $W_\rho(x,y)$ of $|\Psi\rangle = \frac{1}{\sqrt{2}}(|0\rangle + |2\rangle)$, with its marginal $M_\rho(x) = \int dy W_\rho(x,y)$ in the backdrop. (*B*) A fictitious Wigner function $W^{\mathrm{DM1}}(x,y) \equiv M_\rho(x)M_\rho(y)$, with the same distribution $M_\rho(y)$ replicated along the orthogonal axis (red solid curve). (*C*) $W^{\mathrm{DM2}}(x,y) \equiv M_\rho(x)M_{|0\rangle\langle 0|}(y)$, with the vacuum-state distribution $M_{|0\rangle\langle 0|}(y)$ used (red solid curve). *A–C*, *Bottom* show the corresponding density matrix elements. $W^{\mathrm{DM1}}(x,y)$ and $W^{\mathrm{DM2}}(x,y)$ in *B* and *C* do not represent any physical states, confirming the nonclassicality of $|\Psi\rangle$.

Non-Gaussian states. More importantly, we now address non-Gaussian states. Every finite-dimensional state (FDS) in Fock basis, that is, $\rho = \sum_{j,k=0}^{N} \rho_{jk}|j\rangle\langle k|$, is nonclassical, because all coherent states (except vacuum), and their mixtures as well, have an extension to infinite Fock states. It is nontrivial to demonstrate the nonclassicality of FDS when one has access to limited information; for example, a noisy state $f|0\rangle\langle 0| + (1-f)|1\rangle\langle 1|$ for $f \geq \frac{1}{2}$ has no simple signatures of nonclassicality like squeezing and negativity of Wigner function. We prove that our DMs are able to detect all non-Gaussian states in finite dimension of any size, with details in *SI Appendix*, section S4. The essence of our proof is that there always exists a submatrix of the density operator corresponding to DMs, which is not positive definite. Remarkably, this nonpositivity emerges for a marginal distribution along an arbitrary direction, which means that the nonclassicality of FDS is confirmed regardless of the quadrature axis measured, just like the phase-randomized Gaussian states introduced in *SI Appendix*. This makes our DM test experimentally favorable, whereas the degree of negativity may well depend on the quadrature axis except in rotationally symmetric states. Our criteria can further be extended to non-Gaussian states in infinite dimension, particularly those without squeezing effect (*SI Appendix*).

As an illustration, we show the case of a FDS $|\Psi\rangle = \frac{1}{\sqrt{2}}(|0\rangle + |2\rangle)$, whose original Wigner function and matrix elements are displayed in Fig. 1*A*. Our DM methods yield matrix elements as shown in Fig. 1*B* and *C*. The nonpositivity of the density operator is then demonstrated by, for example, $\langle 0|\rho|0\rangle\langle 8|\rho|8\rangle - |\langle 0|\rho|8\rangle|^2 < 0$ under DM1 and $\langle 0|\rho|0\rangle\langle 4|\rho|4\rangle - |\langle 0|\rho|4\rangle|^2 < 0$ under DM2, respectively.

Nonclassicality Measure and Entanglement Potential. We may define a measure of nonclassicality using our DMs as

$$\mathcal{N}_{\mathrm{DM}}(\rho) \equiv \max_{\theta\in(0,\pi)} \frac{||\rho^{\theta}_{\mathrm{DM}}||_1 - 1}{2}, \qquad [6]$$

where $||\cdot||_1$ is a trace norm and $\rho^{\theta}_{\mathrm{DM}}$ a density matrix under DM, using a marginal distribution at angle θ. Our DM negativity possesses the following properties appropriate as a nonclassicality measure, with details in *SI Appendix*: (*i*) $\mathcal{N}_{\mathrm{DM}} = 0$ for a classical state; (*ii*) convex, that is, nonincreasing via mixing states, $\mathcal{N}_{\mathrm{DM}}(\sum_j p_j\rho_j) \leq \sum_j p_j \mathcal{N}_{\mathrm{DM}}(\rho_j)$; and (*iii*) invariant under a classicality-preserving unitary operation, $\mathcal{N}_{\mathrm{DM}}(\hat{U}_c\rho\hat{U}_c^{\dagger}) = \mathcal{N}_{\mathrm{DM}}(\rho)$, where $\hat{U}_c$ refers to displacement or phase rotation. Combining *ii* and *iii*, we also deduce the property that (*iv*) $\mathcal{N}_{\mathrm{DM}}$ does not increase under generic classicality-preserving operations (mixture of unitary operations).

Our nonclassicality measure also makes a significant connection to entanglement potential as follows. A prototypical scheme to generate a CV entangled state is to inject a single-mode nonclassical state into a beam splitter (BS) (20–23). It is important to know the property of those entangled states under partial transposition (PT), which bears on the distillibility of the output to achieve higher entanglement. Our formalism makes a connection between nonclassicality of single-mode resources and NPT of output entangled states. The effect of PT in phase space is to change the sign of momentum, $W_{\rho_{12}}(q_1,p_1,q_2,p_2) \to W_{\rho_{12}}(q_1,p_1,q_2,-p_2)$. If the resulting Wigner function is unphysical, the state ρ_{12} is NPT. We first show that all nonclassical states detected under our DMs can generate NPT entanglement via a BS setting.

We inject a single-mode state ρ and its rotated version $\overline{\rho} = e^{i\frac{\pi}{2}\hat{n}}\rho e^{-i\frac{\pi}{2}\hat{n}}$ into a 50:50 BS, described as

$$W_\rho(q_1,p_1)\,W_{\overline{\rho}}(q_2,p_2) \xrightarrow{\mathrm{BS}} W_\rho\left(\frac{q_1+q_2}{\sqrt{2}},\frac{p_1+p_2}{\sqrt{2}}\right) W_{\overline{\rho}}\left(\frac{q_1-q_2}{\sqrt{2}},\frac{p_1-p_2}{\sqrt{2}}\right). \qquad [7]$$

Applying PT on mode 2 and injecting the state again into a 50:50 BS, we have

$$W_\rho\left(\frac{q_1+q_2}{\sqrt{2}},\frac{p_1-p_2}{\sqrt{2}}\right) W_{\overline{\rho}}\left(\frac{q_1-q_2}{\sqrt{2}},\frac{p_1+p_2}{\sqrt{2}}\right) \xrightarrow{\mathrm{BS}} W_\rho(q_1,p_2)\,W_{\overline{\rho}}(q_2,p_1) = W_\rho(q_1,p_2)\,W_\rho(p_1,q_2). \qquad [8]$$

Integrating over q_2 and p_2, the marginal Wigner function for mode 1 is given by $M_\rho(q_1)M_\rho(p_1)$, which is identical to DM1 of the state ρ in Eq. **1**. The other DM2 in Eq. **2** emerges when replacing the second input state $\overline{\rho}$ by a vacuum $\overline{\rho} = |0\rangle\langle 0|$. Therefore, if the original state ρ is nonclassical under our DMs, the output entangled state via the BS scheme must be NPT.

In ref. 20, single-mode nonclassicality is characterized by entanglement potential via a BS setting, where a vacuum is used as an ancillary input to BS to generate entanglement. We may take negativity, instead of logarithmic negativity in ref. 20, as a measure of entanglement potential; that is,

$$\mathcal{P}_{\mathrm{ent}}[\rho] \equiv \frac{||[\hat{U}_{\mathrm{BS}}(\rho_1 \otimes |0\rangle\langle 0|_2)\,\hat{U}_{\mathrm{BS}}^{\dagger}]^{\mathrm{PT}}||_1 - 1}{2}, \qquad [9]$$

where $\hat{U}_{\mathrm{BS}}$ and $[\cdot]^{\mathrm{PT}}$ represent 50:50 BS operation and partial transpose on mode 2, respectively. We then prove in *SI Appendix* that our DM2 measure provides a lower bound for the entanglement potential as

$$\mathcal{N}_{\mathrm{DM2}}[\rho] \leq \mathcal{P}_{\mathrm{ent}}[\rho]. \qquad [10]$$

Thus, the nonclassicality measured under our framework indicates the degree of entanglement achievable via BS setting.

Experiment

We experimentally illustrate the power of our approach by detecting nonclassicality of several motional states of a trapped $^{171}Yb^{+}$ ion. For the manipulation of motional state, the single phonon-mode $\hat{a}$ along the X direction in 3D harmonic potential with trap frequencies $(\omega_{\mathrm{X}},\omega_{\mathrm{Y}},\omega_{\mathrm{Z}}) = 2\pi\,(2.8, 3.2, 0.6)$ MHz is coupled to two internal levels of the $S_{1/2}$ ground-state manifold, $|F=1, m_F=0\rangle \equiv |\uparrow\rangle$ and $|F=0, m_F=0\rangle \equiv |\downarrow\rangle$ with transition frequency $\omega_{\mathrm{HF}} = (2\pi)\ 12.642821$ GHz. We implement the anti-Jaynes–Cummings interaction $H_{\mathrm{aJC}} = \frac{\eta\Omega}{2}\hat{a}^{\dagger}\hat{\sigma}_{+} + \mathrm{h.c.}$ and the Jaynes–Cummings interaction $H_{\mathrm{JC}} = \frac{\eta\Omega}{2}\hat{a}\hat{\sigma}_{+} + \mathrm{h.c.}$ with $\sigma_{+} = |\uparrow\rangle\langle\downarrow|$. H_{aJC} is realized by two counterpropagating laser beams with beat frequency near $\omega_{\mathrm{HF}} + \omega_{\mathrm{X}}$ and H_{JC} with frequency near $\omega_{\mathrm{HF}} - \omega_{\mathrm{X}}$ (7). $\eta = \Delta k\sqrt{\hbar/2M\omega_{\mathrm{X}}}$ is the Lamb–Dicke parameter, Ω the Rabi frequency of internal transition, Δk the net wave vector of the Raman laser beams, and M the ion mass.

For our test, we generate the Fock states $|n=1\rangle$ and $|n=2\rangle$, together with the ground state $|n=0\rangle$. First, we prepare the ground state by applying the standard Doppler cooling and the Raman sideband cooling. Then we produce the Fock states by a successive application of the π pulse of H_{aJC}, transferring the state $|\downarrow, n\rangle$ to $|\uparrow, n+1\rangle$, and the π pulse for internal state transition $|\uparrow, n+1\rangle$ to $|\downarrow, n+1\rangle$. We also generate a superposition state $\frac{1}{\sqrt{2}}(|0\rangle + |2\rangle)$ by applying the $\pi/2$ pulse of H_{aJC} and then the π pulse of H_{JC}.

Nonclassicality Test. We measure a characteristic function $C_\rho(k_\theta) \equiv \langle e^{-2ik\hat{x}_\theta}\rangle$ with $\hat{x}_\theta = \hat{x}\cos\theta + \hat{p}\sin\theta$, by first making the evolution $\hat{U} = e^{-ik\hat{x}_\theta\hat{\sigma}_x}$ (simultaneously applying H_{aJC} and H_{JC} with proper phases) and then measuring internal state $\hat{\sigma}_z = |\uparrow\rangle\langle\uparrow| - |\downarrow\rangle\langle\downarrow|$ at times t_i $(k = \eta\Omega t)$ (45, 46). Using $\hat{U}^{\dagger}\hat{\sigma}_z\hat{U} = \cos(2k\hat{x}_\theta)\hat{\sigma}_z + \sin(2k\hat{x}_\theta)\hat{\sigma}_y$, we obtain $\langle\cos(2k\hat{x}_\theta)\rangle$ and $\langle\sin(2k\hat{x}_\theta)\rangle$, with the internal state initially prepared in the eigenstates $|+\rangle_z$ and $|+\rangle_y$ of σ_z and σ_y, respectively. The Fourier transform of $C_\rho(k_\theta)$ gives the marginal distribution of $\hat{x}_\theta$ (45, 46). In contrast, we directly use it without

PHYSICS

the Fourier transform, for which our DMs work equally well as for the Wigner function. We test $C^{\mathrm{DM1}} \equiv C_\rho(k_x)C_\rho(k_y)$ or $C^{\mathrm{DM2}} \equiv C_\rho(k_x)C_{|0\rangle\langle 0|}(k_y) = C_\rho(k_x)e^{-\frac{1}{2}\lambda_{k_y}^2}$, with its density operator $\rho = \frac{1}{\pi}\int dk_x\, dk_y\, C(k_x,k_y)\hat{D}^\dagger(k_x,k_y)$ unphysical for a nonclassical state.

To set a benchmark (noise level) for classical states, we prepared the motional ground state $|n=0\rangle$ and obtained its marginal distributions along six axes with 1,000 repetitions for each time t_i. It yielded the negativity $\mathcal{N}_{\mathrm{DM2}} = 0.019 \pm 0.02$ represented by gray shading in Fig. 2 (*SI Appendix*). On the other hand, the Fock states $|n=1\rangle$ and $|n=2\rangle$ clearly manifest nonclassicality for each marginal distribution taken at three different angles θ in Fig. 2*A*, at much higher negativity with error bars considering finite data of 1,000. To further show that our method works regardless of measured axis, we also tested a superposition state $\frac{1}{\sqrt{2}}(|0\rangle + |2\rangle)$ not rotationally symmetric in phase space. As shown in Fig. 2*B*, its nonclassicality is well demonstrated for all measured angles individually whereas the degree of negativity varies with the measured axis.

Compared with our DM, one might look into nonclassicality directly via deconvolution, that is, examine whether a marginal distribution $P(x)$ can be written as a sum of coherent-state distributions as $P(x) = \sqrt{\frac{2}{\pi}}\int d\tilde{x}\tilde{P}(\tilde{x})e^{-2(x-\tilde{x})^2}$, where $\tilde{P}(\tilde{x})$ must be positive definite for classical states. $\tilde{P}(\tilde{x})$ is nothing but the marginal of Glauber–Sudarshan P function and thus typically ill-behaved. One can test the positivity of $\tilde{P}(\tilde{x})$ alternatively using an $n \times n$-moment matrix with elements $M_{ij} \equiv \langle \tilde{x}^{i+j}\rangle$ $(i,j = 0,\ldots,n-1)$ (47). Fig. 2 *C* and *D* shows the results under deconvolution, using the same experimental data as in Fig. 2 *A* and *B*. To confirm nonclassicality, the degree of negativity must be large enough to beat that of the vacuum state, including the statistical errors. Although those states produce negativity under deconvolution, their statistical errors substantially overlap with that of the vacuum state, providing much weaker evidence of nonclassicality than our DM. Full details are given in *SI Appendix*.

Instead of using an entire characteristic function, we can also test our criterion by examining a subset of data using the Kastler–Loupias–Miracle–Sole (KLM) condition (48–51). This simple test provides clear evidence of nonclassicality against experimental imperfections, for example, coarse graining and finite-data acquisition in other experimental platforms as well. The KLM condition states that the characteristic function $C_\rho(\xi) \equiv \mathrm{tr}[\rho\tilde{D}(\xi)]$ for a legitimate quantum state must yield an $n \times n$ positive matrix $\mathcal{M} > 0$ with matrix elements

$$\mathcal{M}_{jk} = C(\xi_j - \xi_k)e^{\frac{1}{2}(\xi_j\xi_k^* - \xi_j^*\xi_k)}, \qquad [11]$$

for an arbitrary set of complex variables $\{\xi_1, \xi_2, \ldots, \xi_n\}$. In our case, we test the positivity of a matrix $(n = 9)$ constructed using 3×3 points of rectangular lattice of size d for the characteristic function under DM2 (*SI Appendix*). As shown in Fig. 3*A*, the ground state $|0\rangle$ shows nonnegativity (and thus the mixture of coherent states as well due to convexity of our method) for all values of d, whereas a nonclassical state $|\Psi\rangle = \frac{1}{\sqrt{2}}(|0\rangle + |2\rangle)$

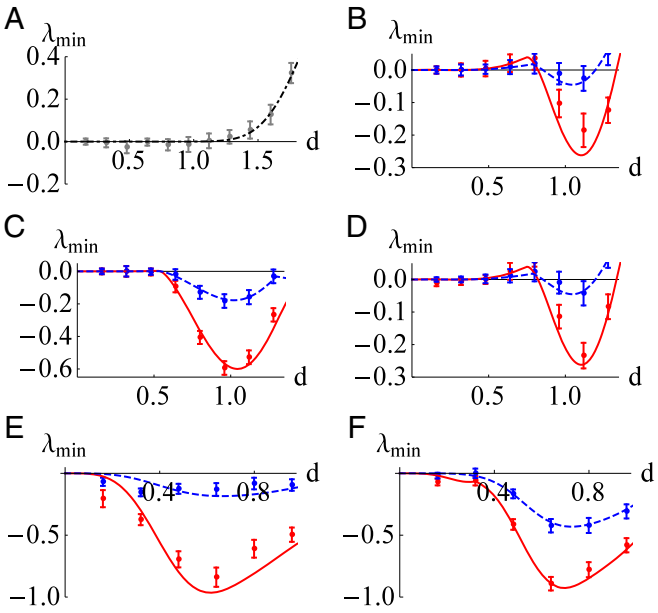

Fig. 3. KLM test under DM2 using a matrix of 3×3 (*A–D*) and 5×5 (*E* and *F*) lattice points, respectively, with $\lambda_{\min}$ the lowest eigenvalue for each lattice size d (*SI Appendix*). Negative $\lambda_{\min}$ manifests the nonclassicality of the considered state. Solid (pure-state $|\Psi\rangle$) and dashed (mixed-state $f|0\rangle\langle 0| + (1-f)|\Psi\rangle\langle\Psi|$) curves represent theoretical predictions and bullets with error bars represent experimental data. (*A*) motional ground state $|0\rangle$. (*B–D*) $|\Psi\rangle = \frac{1}{\sqrt{2}}(|0\rangle + |2\rangle)$ for the measured angles at $\theta = \frac{\pi}{3}$, $\frac{\pi}{2}$, and $\frac{2\pi}{3}$, respectively. (*E*) Fock state $|1\rangle$. (*F*) Fock state $|2\rangle$. For mixed states (dashed curves), we use $f = 0.66$ in *B–D* and $f = 0.5$ in *E* and *F*, respectively.

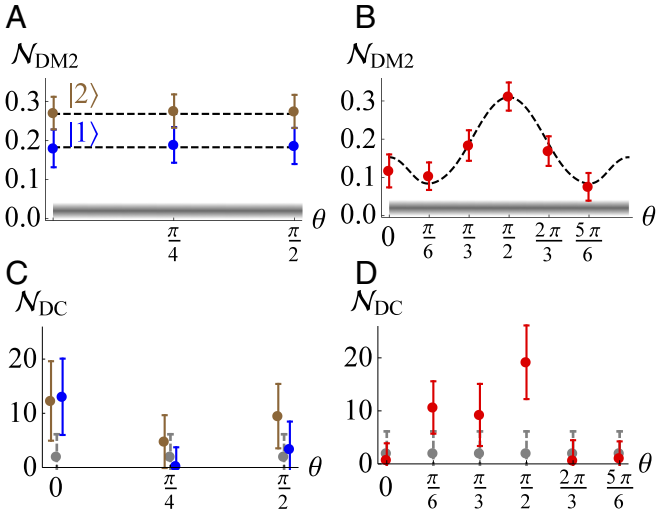

Fig. 2. (*A* and *B*) DM2 negativity against θ of the measured distribution $\langle e^{-2ik\hat{x}_\theta}\rangle$ for (*A*) Fock states $|1\rangle$ and $|2\rangle$ and (*B*) a superposition $\frac{1}{\sqrt{2}}(|0\rangle + |2\rangle)$. Dashed lines, theoretical value; bullets with error bars, experiment; gray shading, noise level for classical states. (*C* and *D*) Negativity under deconvolution test for Fock states $|1\rangle$ (blue), $|2\rangle$ (brown), and $\frac{1}{\sqrt{2}}(|0\rangle + |2\rangle)$ (red), together with $|0\rangle$ (gray), using a 5×5-moment matrix.

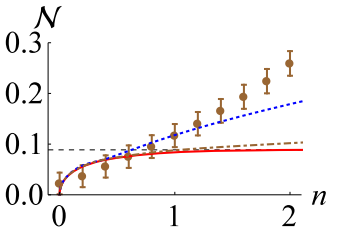

Fig. 4. DM negativity of $f|0\rangle\langle 0| + (1-f)|2\rangle\langle 2|$ (bullets with error bars) from experimental data. Maximum Gaussian negativity under $N = 6$ (blue dotted line), $N = 12$ (brown dotted-dashed line), and $N \to \infty$ (black dashed horizontal line) phase rotations is given against energy n, the negativity above which confirms genuine non-Gaussianity.

manifests negativity in a certain range of d, confirming nonclassicality for each measured distribution at $\theta = \frac{\pi}{3}, \frac{\pi}{2}$, and $\frac{2\pi}{3}$ (red solid curves) in Fig. 3 *B–D*, respectively. Furthermore, note that a mixture of the vacuum and the nonclassical state, $f|0\rangle\langle 0| + (1-f)|\Psi\rangle\langle\Psi|$, possesses a positive-definite Wigner function for $f \geq 0.66$, so even a full tomography may not directly show its nonclassicality via negativity. In contrast, our simple method manifests nonclassicality for $f = 0.66$, shown by blue dashed curves in Fig. 3 *B–D*. For Fock states, we consider the matrix test using 5×5 lattice points, which confirms negativity at the mixing $f = 0.5$ with vacuum giving a nonnegative Wigner function for both states $|1\rangle$ and $|2\rangle$ in Fig. 3 *E* and *F*.

Genuine Non-Gaussianity. We further extend our approach combined with phase randomization to derive a criterion on genuine non-Gaussianity. Notably there exist quantum tasks that cannot be achieved by Gaussian resources, for example, universal quantum computation (52), CV nonlocality test (53, 54), entanglement distillation (55–57), and error correction (58). It is a topic of growing interest to detect genuine non-Gaussianity that cannot be addressed by a mixture of Gaussian states. Previous approaches all address particle nature like the photon-number distribution (59–61) and the number parity in phase space (7, 62, 63) for this purpose. Here we propose a method to examine genuine CV characteristics of marginal distributions. Our criterion can be particularly useful to test a class of non-Gaussian states diagonal in the Fock basis, $\rho = \sum p_n |n\rangle\langle n|$, and thus rotationally symmetric in phase space. For this class, one may detect nonclassicality using photon-number moments (18), which can be experimentally addressed efficiently by phase-averaged quadrature measurements (64, 65). Lvovsky and Shapiro experimentally demonstrated the nonclassicality of a noisy single-photon state $f|0\rangle\langle 0| + (1-f)|1\rangle\langle 1|$ for an arbitrary f (66), using the Vogel criterion (67). In contrast, we look into the genuine non-Gaussianity of non-Gaussian states as follows.

For a Gaussian state $\rho_{\rm G}$, the phase randomization gives $\sigma \equiv \frac{1}{N}\sum_{k=0}^{N-1} e^{-i\theta_k \hat{n}} \rho_{\rm G} e^{i\theta_k \hat{n}}$ with $\theta_k \equiv \frac{k}{N}\pi$. As the number N of phase rotations grows, the DM negativity of Gaussian states decreases. With $N \to \infty$ (full phase randomization), we obtain the Gaussian bound $\mathcal{B}_G \approx 0.0887$ (*SI Appendix*). Thus, if a state manifests a larger DM negativity as $\mathcal{N} > \mathcal{B}_{\rm G}$, it confirms genuine non-Gaussianity. We plot the Gaussian bounds for finite rotations $N = 6$ and $N = 12$ with $\mathcal{B}_{\rm G} \approx 0.0887$ against energy n in Fig. 4. Our data for the state $|2\rangle$, which shows negativity insensitive to measured angles in Fig. 2, indicate genuine non-Gaussianity for the mixed states $f|0\rangle\langle 0| + (1-f)|2\rangle\langle 2|$ with $f = 1 - \frac{n}{2}$. For example, the $N = 12$ case (Fig. 4, brown dotted-dashed line) as well as the full phase randomization (Fig. 4, black dashed horizontal line) confirms quantum non-Gaussianity at $f = \frac{1}{2}$, corresponding to a positive Wigner function.

Conclusion and Remarks

Measuring marginal distributions along different axes in phase space forms a basis of quantum-state tomography with a wide range of applications. A marginal distribution is readily obtained in many different experimental platforms, for example, by an efficient homodyne detection in quantum optical systems (11, 68–71) and by other quadrature measurements in trapped-ion (45, 46, 72), atomic ensembles (73), optomechanics (74, 75), and circuit quantum electrodynamics (QED) systems (76, 77). We here demonstrated that only a single marginal distribution can manifest nonclassicality by using our DMs. Our DM methods are powerful to detect a wide range of nonclassical states, particularly non-Gaussian states. They provide a practical merit with less experimental effort and make a stronger test of nonclassicality by analyzing data without numerical manipulation unlike state tomography.

Remarkably, nonclassicality can be demonstrated regardless of measured quadrature axis for all FDSs, which was also experimentally confirmed using a trapped-ion system. We clearly showed that the proposed method provides a reliable nonclassicality test by directly using a finite number of data, which can be further extended to other CV systems. In addition to the KLM test used here, we can manifest nonclassicality by looking into single marginal distributions under other forms, for example, functional (33) and entropic (78, 79) inequalities. We also extended our approach to introduce a criterion on genuine non-Gaussianity, using marginal distributions combined with a phase-randomization process. Our nonclassicality and non-Gaussianity tests were experimentally shown to successfully detect non-Gaussian states even with positive-definite Wigner functions whose nonclassicality is thus not immediately evident by the tomographic construction of Wigner function. As a remark for those nonclassical states with positive Wigner functions, one may use generalized quasi-probability distributions like a filtered P function (80–82). For example, the experiment in ref. 83 introduced a nonclassicality filter to construct a generalized P function that yields a regularized distribution with negativity as a signature of nonclassicality for the case of photon-added thermal states. On the other hand, our DM method does not require a tomographic construction and provides a faithful test that is reliable against experimental imperfections like finite data and coarse graining.

Moreover, we established the connection between single-mode nonclassicality and NPT entanglement via a BS setting—a prototypical model of producing CV entanglement. The negativity under our DM framework provides a quantitative measure of a useful resource by identifying the minimum level of entanglement achievable in Eq. **10** (as shown in *SI Appendix*, the relation in Eq. **10** holds regardless of the measured axis). Nonclassicality and non-Gaussianity are important resources, making a lot of quantum tasks possible far beyond their classical counterparts. We thus hope our proposed method could provide a valuable experimental tool and a fundamental insight for future studies of CV quantum physics by critically addressing them.

ACKNOWLEDGMENTS. M.S.Z. and H.N. were supported by National Priorities Research Program Grant 8-751-1-157 from the Qatar National Research Fund and K.K. by the National Key Research and Development Program of China under Grants 2016YFA0301900 and 2016YFA0301901 and the National Natural Science Foundation of China under Grants 11374178 and 11574002.

1. Braunstein SL, van Loock P (2005) Quantum information with continuous variables. *Rev Mod Phys* 77:513–577.
2. Cerf NJ, Leuchs G, Polzik ES (2007) *Quantum Information with Continuous Variables of Atoms and Light* (Imperial College, London).
3. Weedbrook C, et al. (2012) Gaussian quantum information. *Rev Mod Phys* 84:621–669.
4. Richter Th, Vogel W (2002) Nonclassicality of quantum states: A hierarchy of observable conditions. *Phys Rev Lett* 89:283601.
5. Ryl S, et al. (2015) Unified nonclassicality criteria. *Phys Rev A* 92:011801(R).
6. Mari A, Kieling K, Nielsen BM, Polzik ES, Eisert J (2011) Directly estimating nonclassicality. *Phys Rev Lett* 106:010403.
7. Park J, et al. (2015) Testing nonclassicality and non-Gaussianity in phase space. *Phys Rev Lett* 114:190402.
8. Park J, Nha H (2015) Demonstrating nonclassicality and non-Gaussianity of single-mode fields: Bell-type tests using generalized phase-space distributions. *Phys Rev A* 92:062134.
9. Glauber RJ (1963) Coherent and incoherent states of the radiation field. *Phys Rev* 131:2766–2788.
10. Sudarshan ECG (1963) Equivalence of semiclassical and quantum mechanical descriptions of statistical light beams. *Phys Rev Lett* 10:277–279.
11. Lvovsky AI, Raymer MG (2009) Continuous-variable optical quantum-state tomography. *Rev Mod Phys* 81:299–332.
12. D'Ariano GM, Macchiavello C, Paris MGA (1994) Detection of the density matrix through optical homodyne tomography without filtered back projection. *Phys Rev A* 50:4298–4302.
13. Hradil Z (1997) Quantum-state estimation. *Phys Rev A* 55:R1561–R1564.

14. Banaszek K, D'Ariano GM, Paris MGA, Sacchi MF (1999) Maximum-likelihood estimation of the density matrix. *Phys Rev A* 61:010304(R).
15. Řeháček J, Mogilevtsev D, Hradil Z (2010) Operational tomography: Fitting of data patterns. *Phys Rev Lett* 105:010402.
16. Teo YS, Zhu H, Englert B-G, Řeháček J, Hradil Z (2011) Quantum-state reconstruction by maximizing likelihood and entropy. *Phys Rev Lett* 107:020404.
17. Shchukin E, Richter Th, Vogel W (2005) Nonclassicality criteria in terms of moments. *Phys Rev A* 71:011802(R).
18. Shchukin EV, Vogel W (2005) Nonclassical moments and their measurement. *Phys Rev A* 72:043808.
19. Bednorz A, Belzig W (2011) Fourth moments reveal the negativity of the Wigner function. *Phys Rev A* 83:052113.
20. Asbóth JK, Calsamiglia J, Ritsch H (2005) Computable measure of nonclassicality for light. *Phys Rev Lett* 94:173602.
21. Kim MS, Son W, Bužek V, Knight PL (2002) Entanglement by a beam splitter: Nonclassicality as a prerequisite for entanglement. *Phys Rev A* 65:032323.
22. Xiang-bin W (2002) Theorem for the beam-splitter entangler. *Phys Rev A* 66:024303.
23. Tahira R, Ikram M, Nha H, Zubairy MS (2009) Entanglement of Gaussian states using a beam splitter. *Phys Rev A* 79:023816.
24. Peres A (1996) Separability criterion for density matrices. *Phys Rev Lett* 77:1413–1415.
25. Horodecki M, Horodecki P, Horodecki R (1996) Separability of mixed states: Necessary and sufficient conditions. *Phys Lett A* 223:1–8.
26. Duan L-M, Giedke G, Cirac JI, Zoller P (2000) Inseparability criterion for continuous variable systems. *Phys Rev Lett* 84:2722–2725.
27. Simon R (2000) Peres-Horodecki separability criterion for continuous variable systems. *Phys Rev Lett* 84:2726–2729.
28. Shchukin E, Vogel W (2005) Inseparability criteria for continuous bipartite quantum states. *Phys Rev Lett* 95:230502.
29. Miranowicz A, Piani M, Horodecki P, Horodecki R (2009) Inseparability criteria based on matrices of moments. *Phys Rev A* 80:052303.
30. Walborn SP, Taketani BG, Salles A, Toscano F, Filho RLM (2009) Entropic entanglement criteria for continuous variables. *Phys Rev Lett* 103:160505.
31. Saboia A, Toscano F, Walborn SP (2011) Family of continuous-variable entanglement criteria using general entropy functions. *Phys Rev A* 83:032307.
32. Nha H, Zubairy MS (2008) Uncertainty inequalities as entanglement criteria for negative partial-transpose states. *Phys Rev Lett* 101:130402.
33. Nha H, Lee S-Y, Ji S-W, Kim MS (2012) Efficient entanglement criteria beyond Gaussian limits using Gaussian measurements. *Phys Rev Lett* 108:030503.
34. Horodecki M, Horodecki P, Horodecki R (1998) Mixed-state entanglement and distillation: Is there a "bound" entanglement in nature? *Phys Rev Lett* 80:5239–5242.
35. Peres A (1999) All the Bell inequalities. *Found Phys* 29:589–614.
36. Dür W (2001) Multipartite bound entangled states that violate Bell's inequality. *Phys Rev Lett* 87:230402.
37. Acin A (2001) Distillability, Bell inequalities, and multiparticle bound entanglement. *Phys Rev Lett* 88:027901.
38. Masanes L (2006) Asymptotic violation of Bell inequalities and distillability. *Phys Rev Lett* 97:050503.
39. Salles A, Cavalcanti D, Acin A (2008) Quantum nonlocality and partial transposition for continuous-variable systems. *Phys Rev Lett* 101:040404.
40. Sun Q, Nha H, Zubairy MS (2009) Entanglement criteria and nonlocality for multimode continuous-variable systems. *Phys Rev A* 80:020101(R).
41. Vertesi T, Brunner N (2012) Quantum nonlocality does not imply entanglement distillability. *Phys Rev Lett* 108:030403.
42. Vertesi T, Brunner N (2014) Disproving the Peres conjecture by showing Bell nonlocality from bound entanglement. *Nat Commun* 5:5297.
43. Barnett SM, Radmore PM (2003) *Methods in Theoretical Quantum Optics* (Oxford Univ Press, Oxford).
44. Scully MO, Zubairy MS (1997) *Quantum Optics* (Cambridge Univ Press, Cambridge, UK).
45. Gerritsma R, et al. (2010) Quantum simulation of the Dirac equation. *Nature* 463:68–71.
46. Gerritsma R, et al. (2011) Quantum simulation of the Klein paradox with trapped ions. *Phys Rev Lett* 106:060503.
47. Agarwal GS (1993) Nonclassical characteristics of the marginals for the radiation field. *Opt Commun* 95:109–112.
48. Kastler D (1965) The C*-algebras of a free Boson field. *Commun Math Phys* 1:14–48.
49. Loupias G, Miracle-Sole S (1966) C*-algebra of canonical systems I. *Commun Math Phys* 2:31–48.
50. Loupias G, Miracle-Sole S (1967) C*-algebra of canonical systems II. *Ann Inst H Poincaré A* 6:39.
51. Nha H (2008) Complete conditions for legitimate Wigner distributions. *Phys Rev A* 78:012103.
52. Lloyd S, Braunstein SL (1999) Quantum computation over continuous variables. *Phys Rev Lett* 82:1784–1787.
53. Nha H, Carmichael HJ (2004) Proposed test of quantum nonlocality for continuous variables. *Phys Rev Lett* 93:020401.
54. García-Patrón R, et al. (2004) Proposal for a loophole-free Bell test using homodyne detection. *Phys Rev Lett* 93:130409.
55. Eisert J, Scheel S, Plenio MB (2002) Distilling Gaussian states with Gaussian operations is impossible. *Phys Rev Lett* 89:137903.
56. Fiurášek J (2002) Gaussian transformations and distillation of entangled Gaussian states. *Phys Rev Lett* 89:137904.
57. Giedke G, Cirac JI (2002) Characterization of Gaussian operations and distillation of Gaussian states. *Phys Rev A* 66:032316.
58. Niset J, Fiurášek J, Cerf NJ (2009) No-go theorem for Gaussian quantum error correction. *Phys Rev Lett* 102:120501.
59. Filip R, Mišta L (2011) Detecting quantum states with a positive Wigner function beyond mixtures of Gaussian states. *Phys Rev Lett* 106:200401.
60. Ježek M, et al. (2011) Experimental test of the quantum non-Gaussian character of a heralded single-photon state. *Phys Rev Lett* 107:213602.
61. Straka I, et al. (2014) Quantum non-Gaussian depth of single-photon states. *Phys Rev Lett* 113:223603.
62. Genoni MG, et al. (2013) Detecting quantum non-Gaussianity via the Wigner function. *Phys Rev A* 87:062104.
63. Hughes C, Genoni MG, Tufarelli T, Paris MGA, Kim MS (2014) Quantum non-Gaussianity witnesses in phase space. *Phys Rev A* 90:013810.
64. Munroe M, Boggavarapu D, Anderson ME, Raymer MG (1995) Photon-number statistics from the phase-averaged quadrature-field distribution: Theory and ultrafast measurement. *Phys Rev A* 52:R924–R927.
65. Banaszek K, Wódkiewicz K (1997) Operational theory of homodyne detection. *Phys Rev A* 55:3117–3123.
66. Lvovsky AI, Shapiro JH (2002) Nonclassical character of statistical mixtures of the single-photon and vacuum optical states. *Phys Rev A* 65:033830.
67. Vogel W (2000) Nonclassical states: An observable criterion. *Phys Rev Lett* 84:1849–1852.
68. Lvovsky AI, et al. (2001) Quantum state reconstruction of the single-photon Fock state. *Phys Rev Lett* 87:050402.
69. Ourjoumtsev A, Tualle-Brouri R, Grangier P (2006) Quantum homodyne tomography of a two-photon Fock state. *Phys Rev Lett* 96:213601.
70. Huisman SR, et al. (2009) Instant single-photon Fock state tomography. *Opt Lett* 34:2739–2741.
71. Cooper M, Wright LJ, Söller C, Smith BJ (2013) Experimental generation of multiphoton Fock states. *Opt Express* 21:5309–5317.
72. Wallentowitz S, Vogel W (1995) Reconstruction of the quantum mechanical state of a trapped ion. *Phys Rev Lett* 75:2932–2935.
73. Fernholz T, et al. (2008) Spin squeezing of atomic ensembles via nuclear-electronic spin entanglement. *Phys Rev Lett* 101:073601.
74. Hertzberg JB, et al. (2010) Back-action-evading measurements of nanomechanical motion. *Nat Phys* 6:213–217.
75. Vanner MR, Hofer J, Cole GD, Aspelmeyer M (2013) Cooling-by-measurement and mechanical state tomography via pulsed optomechanics. *Nat Commun* 4:2295.
76. Mallet F, et al. (2011) Quantum state tomography of an itinerant squeezed microwave field. *Phys Rev Lett* 106:220502.
77. Eichler C, et al. (2011) Experimental state tomography of itinerant single microwave photons. *Phys Rev Lett* 106:220503.
78. Bialynicki-Birula I, Mycielski J (1975) Uncertainty relations for information entropy in wave mechanics. *Commun Math Phys* 44:129–132.
79. Bialynicki-Birula I (2006) Formulation of the uncertainty relations in terms of the Rényi entropies. *Phys Rev A* 74:052101.
80. Agarwal GS, Wolf E (1970) Calculus for functions of noncommuting operators and general phase-space methods in quantum mechanics. I. Mapping theorems and ordering of functions of noncommuting operators. *Phys Rev D* 2:2161–2186.
81. Agarwal GS, Wolf E (1970) Calculus for functions of noncommuting operators and general phase-space methods in quantum mechanics. II. Quantum mechanics in phase space. *Phys Rev D* 2:2187–2205.
82. Agarwal GS, Wolf E (1970) Calculus for functions of noncommuting operators and general phase-space methods in quantum mechanics. III. A generalized Wick theorem and multitime mapping. *Phys Rev D* 2:2206–2225.
83. Kiesel T, Vogel W, Bellini M, Zavatta A (2011) Nonclassicality quasiprobability of single-photon-added thermal states. *Phys Rev A* 83:032116.